Charge transfer in secondary-ion emission: Tight-binding studies in Si and Si:O clusters

M. C. G. Passeggi, E. C. Goldberg, and J. Ferrón
Instituto de Desarrollo Tecnológico para la Industria Química, Güemes 3450, 3000 Santa Fe, Argentina
(Received 16 October 1986)

A cluster tight-binding model is used to compare the ionization probability for Si atoms emitted from a (100) surface in a pure system against that obtained by including an oxygen impurity. Two situations are considered in which the oxygen occupies either a subsurface substitutional site or a site at the surface. The time-dependent dynamical problem is simulated through an exponentially decaying interaction between the ejected atom and the substrate, and the probabilities are found by solving the evolution operator equations in an iterative scheme. We found that the emission of positive and negative Si ion shows an exponential dependence with the inverse of the ejection velocity in a large velocity range, showing a weaker dependence at low velocities. The presence of oxygen enhances the Si^+ emission and suppresses the Si^- emission for the first-neighbor silicon atoms, this effect being strongly localized. For ejected Si atoms not close to the oxygen impurity the effect is smaller and depends on the ejection velocity. In addition, the exponential dependence of Si^--ion emission is strongly altered.

I. INTRODUCTION

Since the introduction of secondary-ion mass spectrometry (SIMS) and ion-scattering spectroscopy (ISS) as two of the most important tools for surface analysis, there has been a growing interest in the basic mechanisms responsible for the final charge states of the particles, either leaving or approaching a solid surface. However, the mechanisms of ion ejection, and mainly the strong enhancement of the ionization probability of sputtered atoms by the presence of oxygen at the surface (one of the most useful effects in SIMS), are still a matter of controversy.[1-4] Thus, we find at present that different models to explain the ion emission from clean[5-9] and contaminated surfaces coexist.[4,10,11] Moreover, it has been suggested that, in some cases, the ion emission of clean metals (intrinsic emission) is produced by the presence of residual oxygen impurities at the surface, explaining in this way the large differences in ion-emission yields observed among elements that oxidize easily, such as Al, Mg, Zr, etc., and inert elements such as Au.[12]

The goal of the different existing models is mainly related to the velocity functional dependence of the ionization probability, and even in this case, the agreement with experimental evidence is only partially fulfilled. In particular, the deviations from the exponential behavior for low sputtered-ion velocities,[13,14] are accounted for in only two cases.[8,15] The enhancement (fall off) of negative (positive) ion emission during the adsorption of electropositive elements[13,16] is explained in all models through modifications of the macroscopic features of the surface, which are quantified through the changes in the target work function (WF model).

On the other hand, the enhancement of both positive- and negative-ion emission yield due to the presence of oxygen at the surface[11] is not explained by these models, since no evident connection with the work function changes is observed.[17,18] The most important models which have intended to rationalize this important SIMS matrix effect, the bond breaking model (BB) and the surface polarization model,[4,10] have never been discussed in other than in a qualitative way.

In this paper we examine the ionization probability for Si atoms ejected from a Si(100) surface, and present quantitative calculations for the oxygen effect on the Si positive-secondary-ion emission. We adopted a description of the atom substrate system based on a cluster of atoms composed by up to 84 atoms. In order to describe the electronic structure in these semiconductor systems we used a tight-binding approach in the first-neighbor approximation with an sp^3s^* basis set per atom, with parameters taken as those which allow for a good reproduction of the band structure of Si and SiO_2 crystals. As the presence of dangling bonds which belong to those boundaries of the cluster other than the surface under examination will introduce fictitious levels on top of the valence band and inside the band gap, we eliminated those dangling orbitals from the basis set. This is a procedure which has been recently used to describe the electronic structure of transition-metal ions and some deep-level defects in Si, producing results[19,20] which are in a fair qualitative agreement with those predictions obtained from more sophisticated calculations.

The dynamical process is simulated by assuming an exponentially time decaying interaction between the ejected atom and the substrate. In this case, the evolution operator can be obtained in a close iterative form which can be solved with a high degree of accuracy.

The organization of the paper is as follows. In Sec. II we briefly analyze the existing models, in Sec. III we present results for the electronic structure of clusters with different atomic configurations. Section IV is devoted to set up the time-dependent scheme used in this paper and in Sec. V we examine and discuss the results for the ionization probabilities including those obtained in the presence of an oxygen impurity. Some concluding remarks are given in Sec. VI.

II. PREVIOUS MODELS

Finite clusters in the one-electron picture have been widely used to represent the solid.[8,21–23] In these cases the electronic part of the system is described by either using a tight-binding approach or a semiempirical LCAO method. A relevant point in these theoretical works is the election of the basis set used to expand the dynamical wave function.[23] The adiabatic molecular states represent the most suitable expansion for just near adiabatic processes as it would be the cases involved in SIMS and ISS processes,[22] provided that no crossing exists along the path between the levels relevant to the ionization process, i.e., the molecular orbitals which evolve into the states of the ejected atom and all those energetically near, which are appreciably coupled to them. Even if these crossing were absent still there is a practical difficulty with this method when applied to a large cluster, for it requires a series of diagonalizations along the ion path to keep track of the evolving states, a procedure which in that case turns to be prohibitedly long as time consumption is concerned. Other microscopic theories start with a time-dependent Anderson-like Hamiltonian (electronic correlation not included) assuming a localized state of energy $E_a(t)$ for the sputtered (scattered) particle, and a time-dependent hopping connecting band states of the substrate with those localized at the adsorbate.[5,9,15,24–28] In this case, the substrate density of states is assumed to be energy independent while $E_a(t)$ is taken from chemisorption calculations and imagelike force considerations.[29]

From a theoretical point of view a great deal of efforts are put in studies of the charge transfer process through the use of the time dependent Anderson-Newns Hamiltonian. This model is quite attractive because it contains in principle the essential ingredients required to examine the relative probabilities for having the sputtered ion in different charge states, depending on the parameters selection. Unfortunately, the dynamical version of this Hamiltonian has been solved exactly only for an extremely small cluster of atoms,[30] although either Hartree-Fock or other approximated solutions have been performed for extended systems thus allowing to keep the problem under tractable form.[31–34] On the other hand, it has been suggested that a one-particle formalism can still be invoked as long as one focus the attention on processes in which the electron transfer occurs either from the atom to the solid or vice versa, treating them as if they were independent processes.[5,26] In the first case the ionization energy of the adatom is used as the free atom parameter, while the affinity level is used to examine the second case, thus allowing for the description of positive- or negative-charged adatom emission, respectively. Indeed, by using the exact solutions obtained in the small-cluster model,[30] it has been shown that this is a reasonable approximation as long as the ionization and the affinity levels of the adatom are far apart. Adopting this point of view, the use of cluster models has received some deal of attention concerning with the mechanisms involved in the SIMS processes.[8,22,23] However, in all cases either the clusters were too small or their selected shapes as linear chains have little resemblance with that one would expect from a solid surface. This in turn makes doubtful whether the effects of impurities on the ionization process can be accounted for by the use of such simplified models.

III. ELECTRONIC STRUCTURE OF THE SELECTED CLUSTERS

The secondary-ion emission from a solid surface is a process which is localized in space and thus amenable to be treated in terms of a portion of the solid. We adopted a cluster whose shape was selected after some trials as to have a level structure that resembles qualitatively the electronic structure of the periodic (100) silicon surface.

The matrix corresponding to the clusters' Hamiltonian were constructed using an empirical tight-binding method (ETBM) within the first-neighbor approximation in a sp^3s^* atomic basis set with parameters given by Vogl *et al.*[35] and Robertson.[36] In order to obtain these matrices we adopted the following procedure. A starting matrix was constructed for a cluster involving 123 atoms (a central one and those corresponding up to the sixth shell of neighbors). The boundaries of these clusters will have dangling bonds coming from the nonsaturated surface atoms, which as stated previously give rise to fictitious effects in the electronic level structure. As our clusters are large enough, these fictitious states will presumably not affect the description of the quite localized ionization process. Therefore, we eliminate the dangling bonds in the form described by Sferco and Passeggi,[20] thus reducing the size of the basis set.

A final matrix for a cluster with the desired shape and having a free surface (retaining its corresponding dangling bonds) was then obtained by "cleaving" the cluster previously obtained with a plane along a fixed direction, suppressing from the actual H matrix all matrix elements coming from atoms being at one of the sides of the free surface. After some trials with "cylindrical rods or slabs" shapes we adopted an "eye-shape" configuration with a free (100) surface including 14 from a total of 84 atoms, and a matrix size of 352×352.

The same shape was used to examine the Si atom ejection in the presence of an oxygen impurity. The first-neighbor Si-O interaction parameters required by the ETBM were taken as those given by Robertson.[36] In all cases the free atom parameters were shifted by a constant amount as to put the top of the valence band fixed at an energy coincident with (minus) the work function of Si, $\phi=-4.87$ eV.[37] The same procedure was used to fix the free oxygen parameters referred to the same energy scale. The parameter set is shown in Table I. Two configurations for the position of the oxygen impurity were selected, as shown schematically in Fig. 1, where 1(a) corresponds to an impurity located within the bulk in a subsurface shell, while in 1(b) the oxygen is located substitutionally at the surface.

The energy level diagram corresponding to these cases are shown in Fig. 2 where the diagram (c) gives the results for a pure silicon cluster. The surface states within the gap spread about 1 eV around the center of the cluster gap. If, as suggested by Sferco and Passeggi, the band edges are located at the values they take in the infinite crystal, some of the levels will remain in the gap, and

TABLE I. Tight-binding parameters used in the present calculations.

	η_{ss}	$\eta_{s_{Si}p_O}$	$\eta_{s_O p_{Si}}$	$\eta_{pp\sigma}$	$\eta_{pp\pi}$	η_{s^*p}	E_s (eV)	E_p (eV)	E_{s^*} (eV)
$d=2.35$ Å Si-Si	−1.508	1.797	1.797	1.971	−0.5218	1.681	−9.07[a]	−3.15[a]	1.68[a]
$d=1.61$ Å Si-O	−1.021	1.837	1.701	2.041	−0.4762	0	−30.25[b]	−15.33[b]	c

Interaction parameters $V_i=\frac{\hbar^2}{md^2}\eta_i$; $\hbar^2/m=7.62$ eV Å^2

[a]Si.
[b]O.
[c]Large number (+).

some of them will merge within the valence band. This is in fair agreement with ETBM results described by Ivanov *et al.*,[38] where for an unreconstructed (100), the surface bridging bonds bands are spread within the gap, and dangling band bonds goes inside the valence band of the bulk. This behavior is more easily recognized when performing a calculation in a larger cluster of 128 atoms (not shown).

The oxygen impurity does not change substantially this picture except in the case of the configuration of Fig. 1(a), where a small change in the position of the last occupied level is produced, thus modifying slightly the work function.

The energy diagram of Fig. 2(c) is that which assumedly resembles the electronic structure of an extended crystal. Obviously, the width of the valence band has not reached the value of the pure crystal, as well as the band gap value is still large, effects which are due to the absence of the long range connectivities of the bonds as they are present in the real crystal.

Once the cluster shape is selected, it is important to consider that the calculation of the ionization probability will require only two diagonalizations of the H matrix for each system. These correspond to two extreme situations for the adatom-substrate interaction: the sputtered atom is part of the solid (initial limit), and the atom is completely decoupled from the solid (asymptotic limit), respectively. This point will be discussed in the next section.

It is important to note that in the tight-binding approximation the free Si p-electron parameters have always higher values than those corresponding to the highest occupied level. Thus, in a strictly adiabatic process, the p states will be completely empty in the asymptotic situation, as electrons from these states would be freely transferred to low-energy states in the solid. In such extremely slow process we will end up with doubly ionized Si atoms. On the other hand, if the ETBM diagonal parameters for the ejected atom are assumed to evolve to values corresponding to the free atom, as long as these parameters end up below the Fermi level of the substrate we would find a final situation with a Si atom charged −4 in a strictly adiabatic process. This is a very unphysical situation which follows from the fact that electron correlation energies are not explicitly included in the model. In order

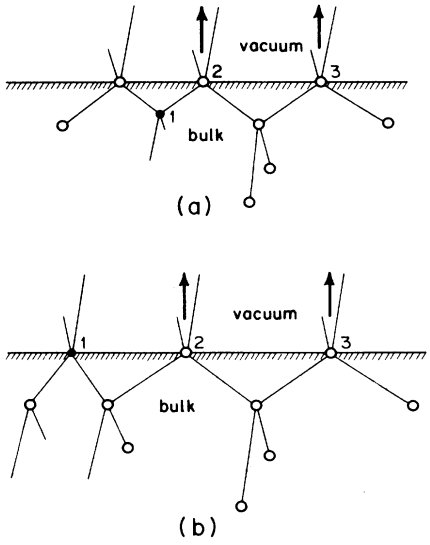

FIG. 1. Schematic view of the [100] surface showing Si atoms which are ejected. Open circles are for Si. Solid circle stands for O. (a) Subsurface oxygen impurity, (b) adsorbed oxygen.

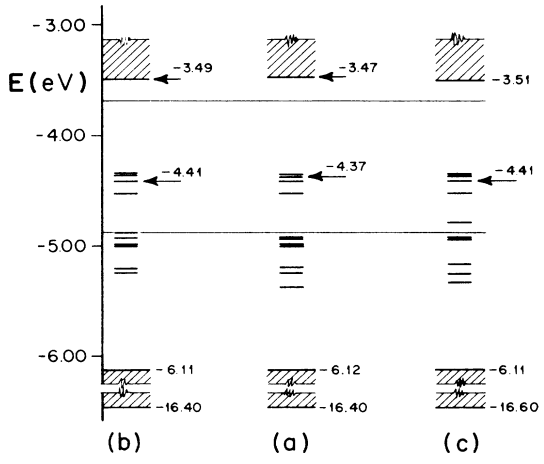

FIG. 2. Energy levels of 84 atom clusters (352 states) showing the band gap region. (a) Corresponds to subsurface oxygen of Fig. 1(a). (b) Adsorbed oxygen [Fig. 1(b)]. (c) Pure silicon cluster. Lines across the three cases show the valence and conduction band edges of setting from a band calculation of Si with parameters of Table I.

to avoid this feature we have allowed only one p-state parameter to vary along the trajectory from its value in the solid to that of the corresponding to the free-atom value[36] referred to a common energy scale.

IV. TIME-DEPENDENT FORMALISM

A. Time evolution

We describe the electronic part of the system through the time-dependent Hamiltonian:

$$H(t)=H_a(t)+H_s+H_1(t) , \tag{1}$$

where

$$H_a(t)=\sum_{i,\sigma}\varepsilon_{ai}(t)a_{i\sigma}^{\dagger}a_{i\sigma} \tag{2}$$

describes the sputtered atom with five states in the s, p_x, p_y, p_z, s^* basis set, $a_{i\sigma}^{\dagger}$ ($a_{i\sigma}$) being their associate creation (anihilation) operators, respectively. As mentioned in Sec. III, we allow for only one p-state diagonal parameter to vary along the trajectory from its value in the solid to the corresponding to the free atom value, with the following assumption:

$$\begin{aligned}&\varepsilon_{ap_z}(t)=(\varepsilon_p-V_0)+V_0e^{-\lambda t}\\&\varepsilon_{ai}(t)=\varepsilon_{ai},\quad i\neq p_z\end{aligned} \tag{3}$$

where ε_{ai} are taken from Table I, V_0 and λ being parameters which characterize the time-decaying energy of the p_z orbital from ε_p to ε_p-V_0.

H_s in Eq. (1) describes the cluster substrate Hamiltonian in terms of the creation and anihilation operators associated with the corresponding molecular orbitals of the substrate:

$$H_s=\sum_{m,\sigma}\varepsilon_m\Psi_{m\sigma}^{\dagger}\Psi_{m\sigma} . \tag{4}$$

The last term in Eq. (1),

$$H_1(t)=\sum_{i,m,\sigma}[V_{im}(t)a_{i\sigma}^{\dagger}\Psi_{m\sigma}+V_{mi}(t)\Psi_{m\sigma}^{\dagger}a_{i\sigma}] , \tag{5}$$

gives the atom-substrate interaction, where the matrix elements are assumed to decay in time as

$$V_{im}(t)=V_{im}(0)e^{-\lambda t} . \tag{6}$$

These matrix elements are obtained from a knowledge of the molecular orbitals (MO's) of the substrate and allowing for a first-neighbor interactions with the sputtered-atom orbitals, as derived by the use of Table I.

The dynamical evolution of the system can be made in terms of the time evolution operator $U(t,t_0)$ defined by the equation of motion ($\hbar=1$):

$$i\frac{\partial U(t,t_0)}{\partial t}=H(t)U(t,t_0) \tag{7}$$

and the condition

$$U(t_0,t_0)=1 .$$

The wave function $\psi(t)$ is obtained from the initial ($t=0$) state $\psi(0)$ as:

$$|\psi(t)\rangle=U(t,t_0)|\psi(0)\rangle . \tag{8}$$

$|\psi(0)\rangle$ is a Slater determinant (even number of electrons) constructed by filling the molecular states Φ_α by increasing order of energies up to the Fermi level of the whole (adatom plus substrate) cluster. These molecular states satisfy

$$H(t=0)\Phi_\alpha=E_\alpha\Phi_\alpha \tag{9}$$

as $H(t)$ is a one-particle Hamiltonian. Therefore,

$$\psi(t)=\det\{\chi_\alpha(t)\}$$

with

$$|\chi_\alpha(t)\rangle=U(t,t_0)|\Phi_\alpha\rangle . \tag{10}$$

Within this scheme, the occupation number $n(t)$ for any state $|a_i\rangle$ centered at the sputtered atom, is given by

$$n_i(t)=2\sum_{\alpha=\text{occ}}|\langle a_i|U(t,0)|\Phi_\alpha\rangle|^2 , \tag{11}$$

with α running over the initially occupied MO's, and the factor of 2 accounts the double occupancy of the orbitals. As a consequence of the normalization of the wave function we have

$$\sum_{\alpha}|\langle a_i|U(t,0)|\Phi_\alpha\rangle|^2=1 , \tag{12}$$

with α now running over the whole set $\{\Phi_\alpha\}$.

B. Transition probabilities

The calculation of the probabilities for different charge states of the sputtered atom is straightforward when the basis set involves an adsorbate described by only one orbital. In such case, and for a spin-independent problem, the knowledge of $n(t)$ allows for the calculation of the final charge-state probabilities. In the case where one electron in the adsorbate represents the neutral configuration, we have

$$\begin{aligned}P^+&=[1-n(\infty)]^2 ,\\P^0&=2[1-n(\infty)]n(\infty) ,\\P^-&=[n(\infty)]^2 ,\end{aligned} \tag{13}$$

as in this case $n(\infty)\uparrow=n(\infty)\downarrow=n(\infty)$, P^0, P^+, and P^- are, respectively, the probabilities of neutral, positive, and negative emission.

In our present case, with five orbitals per site, the selection of all different electronic configurations of the adsorbate which are contained in $\psi(t)$, leading to a specific charge state, becomes more complex. To this end we use operators such as the following:

$$P^{(3)}_{s^2p^1}=\sum_{\sigma=\uparrow,\downarrow;i=p_x,p_y,p_z} n_{s\uparrow}n_{s\downarrow}(1-n_{s^*\uparrow})(1-n_{s^*\downarrow})n_{i\sigma}(1-n_{i-\sigma})\prod_{\delta\,(\neq i)}(1-n_{\delta\uparrow})(1-n_{\delta\downarrow}) , \tag{14}$$

which selects from $\psi(t)$ all the many electron states where the sputtered atom is in a final configuration s^2p^1 irrespective of the occupational scheme of the substrate. Thus, the probability of having a single ionized Si atom is given by

$$P^+(t)=\langle\psi(t)\mid P^{(3)}_{s^2p^1}+P^{(3)}_{s^1p^2}+P^{(3)}_{p^3}\mid\psi(t)\rangle , \tag{15}$$

where we have neglected all those configurations involving the occupancy of the s^* states, as they remain empty along the whole trajectory for the range ejection velocities we have considered. Similarly the probabilities for having a neutral or a negatively charged Si atom are given by

$$P^0(t)=\langle\psi(t)\mid P^{(4)}_{s^2p^2}+P^{(4)}_{sp^3}+P^{(4)}_{p^4}\mid\psi(t)\rangle , \tag{16}$$

$$P^-(t)=\langle\psi(t)\mid P^{(5)}_{s^2p^3}+P^{(5)}_{sp^4}+P^{(5)}_{p^5}\mid\psi(t)\rangle , \tag{17}$$

respectively. Under the selected conditions, the weights of the configurations s^1p^2 and p^3 in Eq. (15) are negligible as compared with that of s^2p^1, and their contributions can be surely ignored. In this case, the explicit expression for P^+ takes the form (see Appendix A)

$$P^+(t)=2\sum_{i=1}^{3}\left[\langle n_{pi}\rangle-\sum_{j\,(\neq i)}\langle n_{pi}n_{pj}\rangle+\langle n_{p1}n_{p2}n_{p3}\rangle\right]\left[1-\sum_{j=1}^{3}\langle n_{pj}\rangle+\sum_{k\,(<j)}\langle n_{pk}n_{pj}\rangle-\langle n_{p1}n_{p2}n_{p3}\rangle\right] , \tag{18}$$

where

$$\begin{aligned}\langle n_{pi}n_{pj}\rangle&=\langle n_{pi}\rangle\langle n_{pj}\rangle-\left|\sum_{\alpha=\mathrm{occ}}\langle a_i\mid U(t,0)\mid\Phi_\alpha\rangle^*\langle\Phi_\alpha\mid U(0,t)\mid a_j\rangle\right|^2\\ \langle n_{p1}n_{p2}n_{p3}\rangle&=\langle n_{p1}\rangle\langle n_{p2}\rangle\langle n_{p3}\rangle-\sum_{i,j,l\;(i\neq j,l)(j\neq l)}\langle n_{pi}\rangle\left|\sum_{\alpha=\mathrm{occ}}\langle a_j\mid U(t,0)\mid\Phi_\alpha\rangle^*\langle\Phi_\alpha\mid U(0,t)\mid a_l\rangle\right|^2\end{aligned} \tag{19}$$

and $\langle n_{pi}\rangle$ is given by Eq. (11) without the prefactor 2.

According to Eqs. (16)–(19) we are requested to know the matrix elements of the evolution operator between the asymptotic states centered at the sputtered atom and the MO's occupied at $t=0$.

$$U_{i\alpha}(t,0)=\langle a_i\mid U(t,0)\mid\Phi_\alpha\rangle . \tag{20}$$

At this point we have to choose the basis set to evaluate the motion Eq. (7). We adopted the MO states corresponding to an infinite separation between the ejected atom and the substrate, which makes the calculation more straightforward. Therefore, we separate $H(t)$ as

$$\begin{aligned}H(t)&=H(\infty)+H'(t) ,\\ H(\infty)&=H_a(\infty)+H_s ,\end{aligned} \tag{21}$$

and

$$H'(t)=V_0e^{-\lambda t}a^\dagger_{p_z}a_{p_z}+H_1(t) . \tag{22}$$

By going now into the interaction picture and defining

$$\tilde{U}(t,0)=e^{iH(\infty)t}U(t,0) . \tag{23}$$

Equation (7) takes the form

$$i\frac{\partial\tilde{U}(t,0)}{\partial t}=\tilde{H}'(t)\tilde{U}(t,0) , \tag{24}$$

with

$$\tilde{H}'(t)=e^{iH(\infty)t}H'(t)e^{-iH(\infty)t} . \tag{25}$$

Using the MO at $t=0$ and those $\{\Phi_i(\infty)\}$ obtained from the asymptotic calculation, we can write Eq. (24) in matricial form as

$$i\frac{\partial}{\partial t}\langle\Phi_i(\infty)\mid\tilde{U}(t,0)\mid\Phi_\alpha\rangle=\sum_k e^{i[E_i(\infty)-E_k(\infty)]t}\langle\Phi_i(\infty)\mid H'(t)\mid\Phi_k(\infty)\rangle\langle\Phi_k(\infty)\mid\tilde{U}(t,0)\mid\Phi_\alpha\rangle , \tag{26}$$

where $H(\infty)\Phi_k(\infty)=E_k(\infty)\Phi_k(\infty)$ and the adsorbate states $\mid a_i\rangle$ belong to the set $\{\Phi_k(\infty)\}$. [$\mid a_i\rangle\equiv\Phi_i(\infty)$, $i=1,2,\ldots,5$].

In connection with Sec. II it is important to remark that the whole calculation requires only two diagonalizations: one at $t=0$ and another at $t=\infty$ to provide for both sets $\{\Phi_\alpha\}$, $\{\Phi_i(\infty)\}$, respectively. The dynamical evolution of the system can be obtained by solving the system of coupled differential Eqs. (26). As in our case there are 352 molecular states this task would be unmanageable. However, according to Eq. (20) we can limit ourselves to the knowledge of only $U_{i\alpha}(\infty,0)$, and because the exponential form assumed for the decaying interaction, the integration can be performed with the result that

an iterative scheme to compute the required matrix elements is obtained (see Appendix B):

$$\tilde{U}_{ai,\alpha}(\infty,0)=e^{i\gamma}\sum_{n=0}^{\infty}\sum_{\beta}A_{ai\beta}^{(n)}\langle\Phi_\beta(\infty)\,|\,\Phi_\alpha(0)\rangle\ ,$$

with

$$A_{ai\beta}^{(n)}=A_{ai\beta}^{(n-1)}\frac{(W_{\beta\beta}-W_{aiai})}{E_{ai}-E_\beta+in\lambda}+\sum_{p}A_{aip}^{(n-1)}\frac{V_{p\beta}}{E_{ai}-E_\beta+in\lambda}\qquad(27)$$

and

$$A_{ai\beta}^{(0)}=\delta_{ai,\beta}\ .$$

Thus, i runs over the five atomic states of the sputtered atom only, whereas β runs over the whole set of 352 asymptotic states. In the present case $W_{ap_zap_z}=V_0=-3.3$ eV, $W_{\beta\beta}=0$ for all $\beta\neq ap_z$. In the previous equation the velocity is introduced by changing t by R/v and taking $\lambda=\sigma v$, where σ is a constant which was taken 2.3 Å^{-1}.[23]

V. NUMERICAL RESULTS AND DISCUSSION

Figure 1 shows schematically the different configurations selected to study the emission of silicon ions. The ejected atoms, (2) and (3) are, respectively, first and third neighbors of the oxygen atom in Fig. 1(a), while in Fig. 1(b), are, respectively, second and fourth neighbors of the oxygen atom. In the case of an infinite pure silicon crystal, both atoms are equivalent. Therefore, the results for pure clusters corresponding to ejection of atoms (2) and (3) were compared in order to check that no boundary effects due to finite cluster size are included in our calculations.

We will now enumerate and discuss the results obtained for the cases mentioned previously.

A. Pure silicon clusters

The plots of $P^{\pm}\equiv P^{\pm}(\infty)$ [Eqs. (15) and (17)] as a function of the inverse of the ion velocity are shown in Fig. 3. These correspond to the ejection of Si atoms located close to the center of the surface [atoms (2) or (3) in Fig. 2], to avoid for cluster edge effects.

The results of P^+ show, at high ion velocities, the typical exponential behavior:[14]

$$P^+\propto\exp(-v_0/v)\ ,$$

with

$$v_0=5.1\times10^{-2}\text{ a.u. }(=1.1\times10^7\text{ cm/s})\ .$$

This value of v_0 is in reasonable agreement with experimental results. Vasile[14] found values of v_0 ranging from 2.3 to 3×10^6 cm/s for several positive emitted ions. Yu[13] found a value of 5×10^6 cm/s for O^- coming from V; and Bayley and MacDonald[39] for Zn^+ in the energy range between 50 and 500 eV found a value of 10^7 cm/s. The value of v_0 is also in agreement with the result of our previous calculations for Al^+ emission from a linear chain cluster ($v_0=7\times10^6$ cm/s), and also with theoretical predictions of Blaise and Nourtier,[3] $v_0\sim1-3\times10^7$ cm/s. For low velocities ($v\lesssim10^{-2}$ a.u.$=2\times10^6$ cm/s), we found a P^+ versus v^{-1} dependence weaker than exponential.

In Fig. 3 we also plotted P^- for a pure silicon cluster. The general trend is similar to the positive emission; i.e., exponential dependence for large velocities with v_0 equals to 1.5×10^7 cm/s, and deviation from the exponential behavior for velocity values lower than 2×10^6 cm/s.

The deviation from the exponential dependence with the inverse of the velocity has been observed experimentally for O^-,[13] and recently for positive ion emission,[14] in the same velocity range. This deviation from the exponential dependence has been attributed to the variation of the ion velocity along the ion path.[15] Adopting this point of view Vasile[14] corrected the measured energies by using an image force term, adjusting the low velocity experimental results to an exponential dependence. However, it has been recently shown that[40] the force required to achieve agreement among experimental results and calculations, would be at least one order of magnitude larger than typical interatomic forces, suggesting that velocity variations along the ion trajectory is not the cause of exponential dependence deviation. In our model calculation, this deviation occurs naturally, although we are assuming a constant velocity along the ion path. We have already pointed out that the deviation effect is in fact due to interferences among the elementary contributions to the transition amplitude along the trajectory.[8] Gagliano *et al.*[23] have also found this type of behavior in a simple linear model whenever the velocity of the sputtered particle goes into a region corresponding to an adiabatic regime. However it would be very difficult to see from our model whether this is situation in our present case.

It is convenient to emphasize here some features about our calculation and the comparisons with experimental results. First, due to the absence of experimental data on emission energy dependence for Si^+, we are comparing

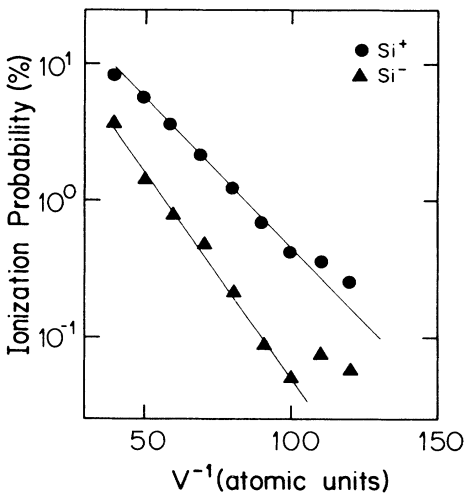

FIG. 3. Ionization probabilities Si^+, Si^- vs inverse of velocity for ions ejected from pure Si clusters.

our calculation with experimental results obtained for different kinds of ions and substrates, i.e., the value of v_0 obtained from our calculation corresponds to a system having a narrow band of surface states, a result of which should not be applicable to metal surfaces. This fact should be kept in mind when making conclusions about our model. Second, the results of P^- should also be taken cautiously, because we are not including any explicit correlation term in the tight-binding Hamiltonian. Although we are using an independent-electron model to describe the solid, we allow for a time-dependent wave function $\psi(t)$ which includes all possible charge configurations of the sputtered atom. It is in this sense that the different charge states are correlated, i.e., to preserve the normalization of $\psi(t)$.

Then, let us compare our calculations with experimental results. Since the slope of both curves P^+ and P^- are similar, we can define a ratio P^+/P^- valid for a wide velocity range, which gives an average value of 6 for this ratio. This is in fair agreement with measurements of Wittmack[4] and Jurela,[41] who obtained values of 3 and 11, respectively, for P^+/P^-.

B. Clusters including oxygen

In order to consider the effect of oxygen on the probabilities P^+ and P^- for silicon atoms, we have analyzed the following cases: oxygen incorporated to the subsurface, first- and third-neighbor silicon atoms sputtered [Fig. 1(a)]; and oxygen adsorbed at the surface, second- and fourth-neighbor silicon atoms sputtered [Fig. 1(b)]. The limitation of the kind of neighbors appears by the combined effects of the surface (100) and the crystalline structure, i.e., there exist no first neighbors belonging to the sample plane (100).

1. *Incorporated oxygen*

Figure 4 shows our results for P^+ in the case of incorporated oxygen [Fig. 1(a)]. As stated above, we limit our calculation to first and third neighbors. We observe a dramatic difference among both types of atoms, revealing the strong localization effect of the oxygen impurity. It is seen that while the first oxygen neighbor increases its ionization probability from a factor of 5 at high velocities, to more than one order of magnitude at lower velocities, the ionization probability for the third neighbor varies only about 20% in the entire velocity range. Moreover, this variation is in the sense of lowering the ionization probability with reference to the pure silicon system. In Fig. 5 we show the velocity dependence of the oxygen effect on the ionization probability (Si^+ oxidized/Si^+ clean). The strong increase in the probability of Si^+ emission is expected on chemical grounds because of the large electron affinity of oxygen, and this is conceptually the basis of the BB model. On the other hand, the lowering of the Si^+ emission produced in the case of the third neighbor cannot be explained by these arguments. These results, however, could be understood on the grounds of the global changes in the electronic structure. Looking at Fig. 2 we observe a slight variation of the silicon work function, being consistent with the lowering of Si^+ emission.

In consequence, we find that the incorporated oxygen may either enhance or lower the Si^+ ion emission depending on the atom location, being these effects of different order of magnitude, as shown in Fig. 5. Certainly, the lowering in the Si^+ emission cannot be measured as it will be shadowed by the strong enhancement produced by oxygen on its nearest Si atom. However, the importance of this result rests on the fact that oxygen, despite its large electron affinity, can according to its proximity of the ejected atom, be able of reducing the positive ion emission. The obvious next question will be about the

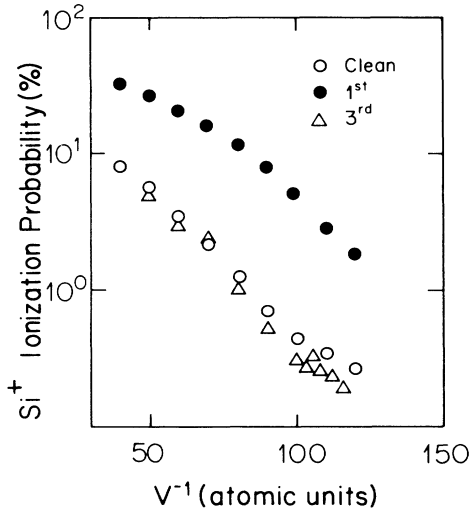

FIG. 4. Ionization probabilities for Si^+ (incorporated oxygen) vs inverse velocity. First and third oxygen neighbors. Results for pure Si cluster are also shown.

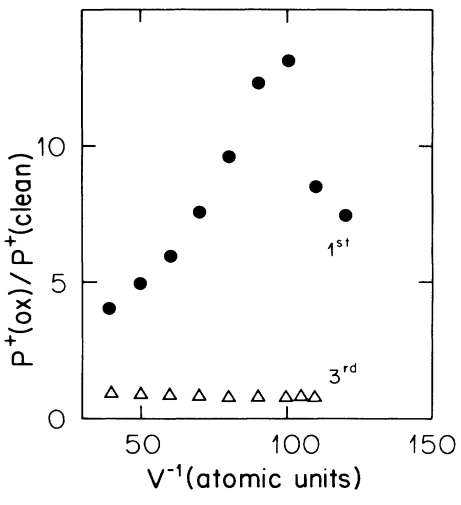

FIG. 5. Ionization probability ratio P^+ (oxid)/P^+ (clean) vs inverse of velocity. First and third oxygen neighbors [atoms 2 and 3 in Fig. 1(a)].

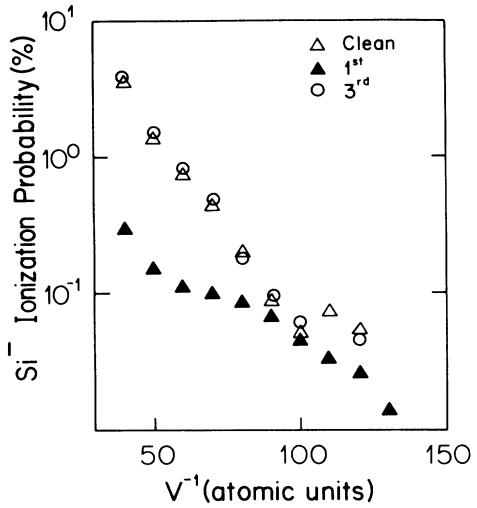

FIG. 6. Si^- ionization probabilities vs inverse of velocity. First and third oxygen neighbors [atoms 2 and 3 of Fig. 1(a)].

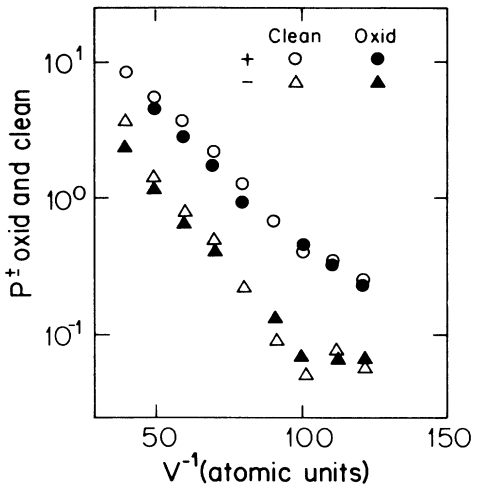

FIG. 8. Ionization probabilities for P^+ and P^- corresponding to atom 2 of Fig. 1(b) vs inverse of velocity. Adsorbed oxygen.

enhancement by oxygen of negative emission, since experimental oxygen enhancement of negative ion emission cannot be explained on the basis of BB model, and within the WF model, only through the surface polarization model.

In Fig. 6 we show the results for Si^- ion emission for the case of incorporated oxygen and for first and third neighbor. As for the positive emission the stronger effect appears for the first neighbor. In this case, the stronger lowering of Si^- emission is observed for the larger velocities, and it is accompanied by a loss of the exponential dependence. Although no direct measurements of velocity dependence of negative Si ion emission in the presence of oxygen have been made, Yu[42] has found that the exponential dependence of O^- is lost in going from clean metal[13] to SiO_x.[42] In Fig. 6, it is also shown the results for the third neighbor. The negative enhancement observed may, as the lowering of Si^+, be explained on the grounds of a global change in the band states. Figure 7 shows the velocity dependence of the oxygen effect on negative emission (Si^- oxidized/Si^- clean). We want to emphasize again that the results for negative emission should be taken cautiously, since no electronic correlation is explicitly included in the model.

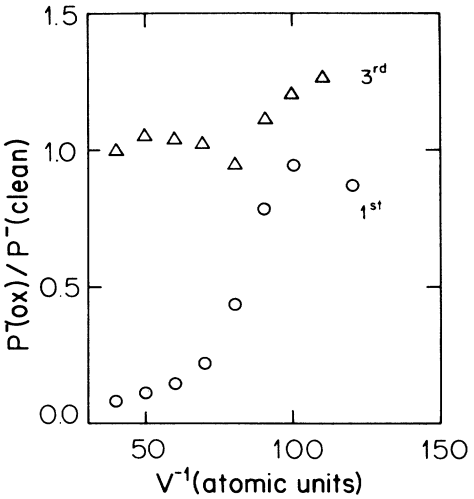

FIG. 7. Ionization probability ratio P^- (oxid)/P^- (clean) vs inverse of velocity. First and third oxygen neighbors. Incorporated oxygen.

2. *Adsorbed oxygen*

In the case of adsorbed oxygen the structure is rather different from the one we have discussed in the previous paragraph. First, for the incorporated oxygen the impurity atom has saturated all its bonds with Si atoms, while the adsorbed oxygen has two dangling bonds. This and the fact that we are simulating the ion emission by quenching its interactions without considering a real motion of the silicon atom, lead us to expect a lower effect of adsorbed oxygen on $Si^{\pm}$ ion emission.

In Fig. 8 we show the results of $Si^{\pm}$ emission probability for the case of adsorbed oxygen and clean silicon. We include only the case of second neighbor since the fourth one does not show any difference with the clean case. As expected, the effect of oxygen, is weaker than its effect as an incorporated impurity, the differences shown in Fig. 3 being at most of 40%. In this case, both positive and negative emission have smaller probabilities, showing an exponential dependence at high velocities and no definite behavior at low velocities. Here, again, no correlation with any of existing models can be made.

CONCLUDING REMARKS

We have calculated the positive- and negative-secondary-ion-emission probability of silicon from a pure substrate, and in the presence of an oxygen impurity. Our results can be summarized as follows.

(i) Positive- and negative-ion emission shows an ex-

ponential dependence with the inverse of the ejection velocity for a wide range of velocities, showing a deviation at the lower velocities.

(ii) The presence of oxygen produces a strong enhancement for the positive emission and a suppression of the negative for ejected atoms closely located to the impurity atom. In addition, the exponential dependence of negative emission is strongly altered.

(iii) The oxygen effect is dependent on the ejection velocity.

(iv) Oxygen has the capability of enhancing or suppressing both types of emission (in different orders of magnitude) depending on the ejection velocity and ejected atom location.

These results support previous suggestions of the coexistence of at least two mechanisms governing the effect of oxygen on the ion emission:[1] one related to the bond-breaking model, and the other to models such as the tunneling one. In our model the importance of each mechanism depends on the distance of the ejected atom to the oxygen impurity.

Since the strongest effect produced by oxygen appears over its near neighbors and is originated in its hig electron affinity, it is reasonable that no correlation exists between Si^+ ion enchancement and the global changes of the electronic structure of silicon due to oxygen, as it was measured recently by Yu and co-workers.[43] On the other hand, our calculations show that the effect of oxygen on Si^- emission depends on the velocity of the ejected atom and on its position relative to the impurity. This fact prevents any prediction *a priori* about the behavior of Si^- emission during oxygen exposure; but it opens the possibility of oxygen of enhancing the Si^- yield, as it has been measured.

ACKNOWLEDGMENTS

The Instituto de Desarrollo Tecnológico para la Industria Quîmica (INTEC) belongs to the Consejo Nacional de Investigaciones Cientîficas y Técnicas (CONICET) and the Universidad Nacional del Litoral, Argentina Financial support from CONICET, under Grant No. 905607 is gratefully acknowledged.

APPENDIX A

In order to calculate the probability amplitude for a given electronic configuration of the ejected atom to be contained in $\psi(t)$ we were required to evaluate matrix elements of the form

$$\langle \psi(t) \mid n_{x\uparrow}(1-n_{x\downarrow})(1-n_{y\uparrow})(1-n_{y\downarrow}) \times (1-n_{z\uparrow})(1-n_{z\downarrow}) \mid \psi(t) \rangle \ . \quad \text{(A1)}$$

Taking into account that atomic states of the ejected atom can be expanded in terms of the $\chi_\alpha(t)$ [Eq. (10)], we can write

$$n_{i\uparrow} = \sum_{\alpha,\beta} \langle \chi_\alpha(t) \mid a_i \rangle \langle a_i \mid \chi_\beta(t) \rangle \chi^\dagger_{\alpha\uparrow} \chi_{\beta\uparrow} \ , \quad \text{(A2)}$$

where the $\chi^\dagger$'s (χ's) are their corresponding creation (annihilation) operators; which are able to operate on the space occupation number which defines $\psi(t)$ at time t. Note also the double sum runs over all α and β.

We thus see that the calculation of any string of n_i's operators as required in Eq. (A1) goes into the calculation of matrix elements of the type

$$\langle \psi(t) \mid \chi^\dagger_{\alpha\uparrow} \chi_{\beta\uparrow}, \ldots, \chi^\dagger_{\delta\downarrow} \chi_{\delta\downarrow} \mid \psi(t) \rangle \ .$$

Since $\psi(t)$ is represented by a single determinant, the indexes α, β, etc. must combine to produce number operators in terms of the $\chi^\dagger$, χ opeators, otherwise the matrix elements will vanish. Also orbital indexes associated with spin-up ($\uparrow$) states cannot be mixed with those of spin down ($\downarrow$). As these indexes are not correlated we can calculate all matrix elements involving spin-up operators separately from those required for spin-down projections.

As an example we can calculate $\langle n_{j\uparrow} n_{k\uparrow} \rangle$ which is given by

$$\begin{aligned}\langle n_{j\uparrow} n_{k\uparrow} \rangle &\equiv \langle \psi(t) \mid n_{j\uparrow} n_{k\uparrow} \mid \psi(t) \rangle \\ &= \sum_{\substack{\alpha,\beta \\ \gamma,\delta}} [\langle \Phi_\alpha \mid U^\dagger(t,0) \mid a_j \rangle \langle a_j \mid U(t,0) \mid \Phi_\beta \rangle \langle \Phi_\gamma \mid U^\dagger(t,0) \mid a_k \rangle \langle a_k \mid U(t,0) \mid \Phi_\delta \rangle] \\ &\quad \times \langle \psi(t) \mid \chi^\dagger_{\alpha\uparrow} \chi_{\beta\uparrow} \chi^\dagger_{\gamma\uparrow} \chi_{\delta\uparrow} \mid \psi(t) \rangle \ .\end{aligned}$$

There are only two possibilities to combine the orbital indexes to get number operators: i.e., $\alpha=\beta$, $\gamma=\delta$ or $\delta=\alpha$, $\beta=\gamma$. Therefore, we get

$$\begin{aligned}\langle n_{j\uparrow} n_{k\uparrow} \rangle = \sum_{\alpha,\gamma=\text{occ}} [&\mid \langle a_j \mid U(t,0) \mid \Phi_\alpha \rangle \mid^2 \mid \langle a_k \mid U(t,0) \mid \Phi_\gamma \rangle \mid^2 \\ &- \langle \Phi_\alpha \mid U^\dagger(t,0) \mid a_j \rangle \langle a_j \mid U(t,0) \mid \Phi_\gamma \rangle \langle \Phi_\gamma \mid U^\dagger(t,0) \mid a_k \rangle \langle a_k \mid U(t,0) \mid \Phi_\alpha \rangle] \ ,\end{aligned}$$

which can easily be reordered to write the result as in Eq. (19).

APPENDIX B

Writing the time-dependent Hamiltonian as

$$H(t) = H(\infty) + V(t) \ , \quad \text{(B1)}$$

we can introduce the evolution operator (with $\hbar=1$):

$$\tilde{U}(t,0) = e^{iH(\infty)} U(t) \ . \quad \text{(B2)}$$

Taking the matrix elements

$$\tilde{U}_{im}(t,0) = \langle \chi_i(\infty) \mid \tilde{U}(t,0) \mid \Phi_n(0) \rangle \ , \quad \text{(B3)}$$

where $\{\chi_i(\infty)\}$ and $\{\Phi_m(0)\}$ are the eigenvectors of $H(\infty)$ and $H(0)$, respectively; we can write the differential equation of motion as

$$\frac{\partial \tilde{U}_{am}(t,0)}{\partial t} = -i \sum_s e^{i\omega_{as}t} V_{as}(t) \tilde{U}_{sm}(t,0) , \tag{B4}$$

with

$$\omega_{as} = \varepsilon_a(\infty) - \varepsilon_s(\infty) \tag{B5}$$

and

$$V_{as}(t) = \begin{cases} e^{-\lambda t} V_{as}, & s \neq a \\ e^{-\lambda t} W_{aa}, & s = 0 . \end{cases}$$

As there are diagonal terms in the time-dependent interaction, it is convenient to make a further phase transformation:

$$\tilde{U}_{am}(t,0) = \exp(i W_{aa} e^{-\lambda t}/\lambda) \bar{U}_{am}(t,0) . \tag{B6}$$

It follows that

$$\begin{aligned} \bar{U}_{am}(0,0) &= e^{-iW_{aa}/\lambda} S_{am} , \\ \bar{U}_{am}(\infty,0) &= \tilde{U}_{am}(\infty,0) , \end{aligned} \tag{B7}$$

being that

$$S_{am} = \langle \chi_a(\infty) \mid \Phi_m(0) \rangle . \tag{B8}$$

Also

$$\frac{\partial \bar{U}_{am}}{\partial t} = -i \sum_{s(\neq a)} V_{as} e^{i(\omega_{as} + i\lambda t)} \phi_{as}(t) \bar{U}_{sm}(t,0) , \tag{B9}$$

where

$$\phi_{as}(t) = \exp[-i(W_{aa} - W_{ss}) e^{-\lambda t}/\lambda] .$$

Integrating (B9), we have

$$\bar{U}_{am}(\infty,0) = e^{-iW_{aa}/\lambda} S_{am} - i \sum_{s(\neq a)} V_{as} \int_0^\infty dt' \, e^{i(\omega_{as} + i\lambda)t'} \phi_{as}(t') \bar{U}_{sm}(t',0) . \tag{B10}$$

The integral in Eq. (B10) can be performed by parts with the result

$$\begin{aligned} \int_0^\infty dt' \, e^{i(\omega_{as} + i\lambda)t'} \phi_{as}(t') \bar{U}_{sm}(t',0) = i \frac{e^{-iW_{aa}/\lambda}}{\omega_{as} + i\lambda} S_m + \frac{1}{\omega_{as} + i\lambda} \Bigg[(W_{ss} - W_{aa}) \int_0^\infty dt' \, e^{i(\omega_{as} + 2i\lambda)t'} \phi_{as}(t') \bar{U}_{sm}(t',0) \\ + \sum_{p(\neq s)} V_{sp} \int_0^\infty dt' \, e^{i(\omega_{ap} + 2i\lambda)t'} \phi_{ap}(t') \bar{U}_{pm}(t',0) \Bigg] . \end{aligned} \tag{B11}$$

This procedure can again be repeated for the integrals on the right-hand side of Eq. (B11), obtaining, finally,

$$\tilde{U}_{am}(\infty,0) = \bar{U}_{am}(\infty,0) = e^{-iW_{aa}/\lambda} \sum_{n=0}^{\infty} \sum_s A_{as}^{(n)} S_{sm} ,$$

with

$$A_{as}^{(n)} = A_{as}^{(n-1)} \frac{(W_{ss} - W_{aa})}{\omega_{as} + in\lambda} + \sum_p A_{ap}^{(n-1)} \frac{V_{ps}}{\omega_{as} + in\lambda}$$

and

$$A_{as}^{(0)} = \delta_{a,s} .$$

[1] P. Williams, Appl. Surf. Sci. **13**, 241 (1982).
[2] P. Williams, Surf. Sci. **90**, 588 (1979).
[3] G. Blaise and A. Nourtier, Surf. Sci. **90**, 496 (1979).
[4] K. Wittmaack; Surf. Sci. **112**, 168 (1981).
[5] J. K. Norskov and B. I. Lundquist, Phys. Rev. B **19**, 5661 (1979).
[6] Z. Sroubek, J. Zavadil, F. Kubec, and K. Zandsky, Surf. Sci. **77**, 603 (1978).
[7] Z. Sroubek, K. Zdansky, and J. Zavadil, Phys. Rev. Lett. **45**, 580 (1980).
[8] E. C. Goldberg, J. Ferrón, and M. C. G. Passeggi, Phys. Rev. B **30**, 2448 (1984).
[9] A. Blandin, A. Nourtier, and D. W. Hone, J. Phys. (Paris) **37**, 309 (1976).
[10] G. Slodzian and J. F. Hennequin, C. R. Acad. Sci. Ser. B **263**, 1246 (1966).
[11] P. Williams and C. A. Evans, Surf. Sci. **78**, 324 (1978).
[12] R. Baragiola, J. Ferrón, and G. Zampieri, Nucl. Instrum. Methods Phys. Res. B **2**, 614 (1984).
[13] M. L. Yu, Phys. Rev. Lett. **47**, 1325 (1981).
[14] M. J. Vasile, Phys. Rev. B **29**, 3785 (1984).
[15] N. D. Lang, Phys. Rev. B **27**, 2019 (1983).
[16] M. L. Yu and N. D. Lang, Phys. Rev. Lett. **50**, 127 (1983).
[17] J. Ferrón, Surf. Sci. Lett. **115**, 275 (1982).
[18] G. Blaise and G. Slodzian, Surf. Sci. **40**, 708 (1973).
[19] M. Gemma, J. Phys. C **17**, 2333 (1984).
[20] S. J. Sferco and M. C. G. Passeggi, J. Phys. C **18**, 3717 (1985).
[21] H. K. McDowell, J. Chem. Phys. **77**, 3203 (1982).
[22] B. J. Garrison, A. C. Diebold, and J. H. Lin, Surf. Sci. **124**, 401 (1983).
[23] E. R. Gagliano, E. C. Goldberg, M. C. G. Passeggi, and J. Ferrón, Phys. Rev. B **31**, 6988 (1985).
[24] Y. Muda and T. Hanawa, Surf. Sci. **97**, 283 (1980).
[25] W. Bloss and D. Hone, Surf. Sci. **72**, 277 (1978).
[26] N. D. Lang and J. K. Norskov, Phys. Scripta **T6**, 15 (1983).
[27] R. Kawai; Phys. Rev. B **32**, 1013 (1984).
[28] K. L. Sebastian, V. C. Jyothi Bhasu, and T. B. Grimley, Surf. Sci. **110**, 2571 (1981).

[29]N. D. Lang and R. Williams, Phys. Rev. B **18**, 616 (1978).
[30]E. C. Goldberg, E. R. Gagliano, and M. C. G. Passeggi; Phys. Rev. B **32**, 4375 (1985).
[31]T. B. Grimley, V. C. Iyothi Bhasu, and K. L. Sebastian, Surf. Sci. **124**, 305 (1983).
[32]K. L. Sebastian, Phys. Lett. **98A**, 39 (1983).
[33]K. L. Sebastian, Phys. Rev. B **31**, 6976 (1985).
[34]R. Brako and D. M. Newns, Solid State Commun. **55**, 633 (1985).
[35]P. Vogl, H. J. Hjalmarson, and J. Dow, J. Phys. Chem. Solids **44**, 365 (1983).
[36]J. Robertson, Adv. Phys. **32**, (1983).
[37]*American Institute of Physics Handbook,* 3rd ed. (McGraw-Hill, New York, 1972).
[38]I. Ivanov, A. Mazur, and J. Pollmann, Surf. Sci. **92**, 365 (1980).
[39]A. R. Bayley and R. J. MacDonald; Radiat. Eff. **34**, 169 (1977).
[40]W. L. Clinton and S. Pal, Phys. Rev. B **33**, 2817 (1986).
[41]Z. Jurela; Radiat. Eff. **13**, 167 (1972).
[42]M. L. Yu, Phys. Rev. B **26**, 4731 (1982).
[43]M. L. Yu, J. Clabes, and D. J. Vitkavage, J. Vac. Sci. Technol. **3**, 1316 (1985).